Structure and Subunit Arrangement of the A-type ATP Synthase Complex from the Archaeon Methanococcus jannaschii Visualized by Electron Microscopy

Coskun, Ünal; Chaban, Yuriy L.; Lingl, Astrid; Müller, Volker; Keegstra, Wilko; Boekema, Egbert J.; Grüber, Gerhard; Gruber, 27460

Published in:
The Journal of Biological Chemistry

DOI:
10.1074/jbc.M406196200

Publication date:
2004

THE JOURNAL OF BIOLOGICAL CHEMISTRY
Vol. 279, No. 37, Issue of September 10, pp. 38644–38648, 2004
Printed in U.S.A.

Structure and Subunit Arrangement of the A-type ATP Synthase Complex from the Archaeon *Methanococcus jannaschii* Visualized by Electron Microscopy*

Received for publication, June 3, 2004
Published, JBC Papers in Press, June 27, 2004, DOI 10.1074/jbc.M406196200

Ünal Coskun‡, Yuriy L. Chaban§, Astrid Lingl¶, Volker Müller¶, Wilko Keegstra§, Egbert J. Boekema§, and Gerhard Grüber‡‖

From the ‡Universität des Saarlandes, Fachrichtung 2.5-Biophysik, D-66421 Homburg, Germany, §Department of Biophysical Chemistry, Groningen Biomolecular Sciences and Biotechnology Institute, University of Groningen Nijenborgh 4, 9747 AG Groningen, The Netherlands, and ¶Institut für Mikrobiologie, Johann Wolfgang Goethe-Universität Frankfurt, D-60439 Frankfurt, Germany

In Archaea, bacteria, and eukarya, ATP provides metabolic energy for energy-dependent processes. It is synthesized by enzymes known as A-type or F-type ATP synthase, which are the smallest rotatory engines in nature (Yoshida, M., Muneyuki, E., and Hisabori, T. (2001) *Nat. Rev. Mol. Cell. Biol.* 2, 669–677; Imamura, H., Nakano, M., Noji, H., Muneyuki, E., Ohkuma, S., Yoshida, M., and Yokoyama, K. (2003) *Proc. Natl. Acad. Sci. U. S. A.* 100, 2312–2315). Here, we report the first projected structure of an intact A_1A_0 ATP synthase from *Methanococcus jannaschii* as determined by electron microscopy and single particle analysis at a resolution of 1.8 nm. The enzyme with an overall length of 25.9 nm is organized in an A_1 headpiece (9.4 × 11.5 nm) and a membrane domain, A_0 (6.4 × 10.6 nm), which are linked by a central stalk with a length of ~8 nm. A part of the central stalk is surrounded by a horizontal-situated rod-like structure ("collar"), which interacts with a peripheral stalk extending from the A_0 domain up to the top of the A_1 portion, and a second structure connecting the collar structure with A_1. Superposition of the three-dimensional reconstruction and the solution structure of the A_1 complex from *Methanosarcina mazei* Gö1 have allowed the projections to be interpreted as the A_1 headpiece, a central and the peripheral stalk, and the integral A_0 domain. Finally, the structural organization of the A_1A_0 complex is discussed in terms of the structural relationship to the related motors, F_1F_0 ATP synthase and V_1V_0 ATPases.

ATP synthases/ATPases are present in every life form and are the most important enzymes for the energy metabolism of the cell (1). They catalyze the formation of ATP at the expense of the transmembrane electrochemical ion gradient. They arose from a common ancestor that underwent structural and functional changes leading to three distinct classes of A_1A_0,[1] F_1F_0, and V_1V_0 ATP synthases/ATPases. The V-type ATPases, found in organelles of eukaryotes, lost their ability to synthesize ATP. Their function is to create steep ion gradients at the expense of ATP hydrolysis (2). Archaea contain ATPases, the A_1A_0 ATP synthases, that are structurally similar to V_1V_0 ATPases but synthesize ATP like the F-type ATPases. The genomic sequences available today show that the overall subunit composition of the A_1A_0 ATP synthases is very similar to the V_1V_0 ATPases. For example, the A_1A_0 ATP synthases contain duplicated and even triplicated K subunits (proteolipids) (3, 4). The A_1A_0 ATP synthase has at least nine subunits ($A_3B_3CDEFHIK_X$), but the actual subunit stoichiometry, especially regarding the proteolipid subunits K in A ATPases, is different in various organisms (12, 6, 4, or as suggested by genomic data, only 1 (5)). The A_1A_0 ATP synthase is composed of a water-soluble A_1 ATPase and an integral membrane subcomplex, A_0. ATP is synthesized or hydrolyzed on the A_1 headpiece consisting of an A_3B_3 domain, and the energy that is provided for or released during that process is transmitted to the membrane-bound A_0 domain (4). The energy coupling between the two active domains occurs via the so-called stalk part, an assembly proposed to be composed of the subunits C, D, and F (6, 7).

Insight in the molecular structure of the A-type ATP synthases comes from small-angle x-ray scattering data of the A_1 ATPase from *Methanosarcina mazei* Gö1 whose A_1 domain is made up of the five different subunits, A_3B_3CDF (8). The data have shown that the hydrated A_1 ATPase is rather elongated with a headpiece of 10 × 9.4 nm in dimension and a stalk of ~8.4 nm in length. A comparison of the central stalk of this A_1 complex with bacterial F_1 and eukaryotic V_1 ATPase indicates different lengths of the stalk domain (8, 9). Image processing of electron micrographs of negatively stained A_1 ATPase from *M. mazei* Gö1 (7) has revealed that the headpiece consists of a pseudohexagonal arrangement of six masses surrounding a seventh mass. These barrel-shaped masses of ~3.2 and 2.8 nm in diameter and 7.5 and 5.0 nm in length, which consist of the major subunits A and B, are arranged in an alternating manner (7). The hexagonal barrel of subunits A and B encloses a cavity of ~2.3 nm in the middle in which part of the central stalk is asymmetrically located. The stalk protrudes from the bottom side of the headpiece forming an angle of ~20° with the vertical axis of the molecule. At the upper end of the hexagonal barrel, extensions can be observed that are assumed to belong to the N termini of subunit A (7). Further insights into the topology of the A_1 ATPase were obtained by differential protease sensitivity (8) and cross-linking studies (6, 7). These studies

* This research was supported by Deutsche Forschungsgemeinschaft Grants GR 1475/9-1 and GR 1475/9-2 (to G. G.) and MU 801/10-3 (to V. M.) and from the Dutch Science Foundation NWO-CW Grant 99009 (to E. J. B.). The costs of publication of this article were defrayed in part by the payment of page charges. This article must therefore be hereby marked "*advertisement*" in accordance with 18 U.S.C. Section 1734 solely to indicate this fact.

‖ To whom correspondence should be addressed: Universität des Saarlandes, FR2.5-Biophysik, Universitätsbau 76, D-66421 Homburg, Germany. Tel.: 49-6841-162-6085; Fax: 49-6841-162-6086; E-mail: ggrueber@uniklinik-saarland.de.

[1] The abbreviations used are: A_1A_0 ATPase, Archaea-type ATPase; F_1F_0, F_1F_0 ATP synthase; V_1V_0 ATPase, vacuolar-type ATPase.

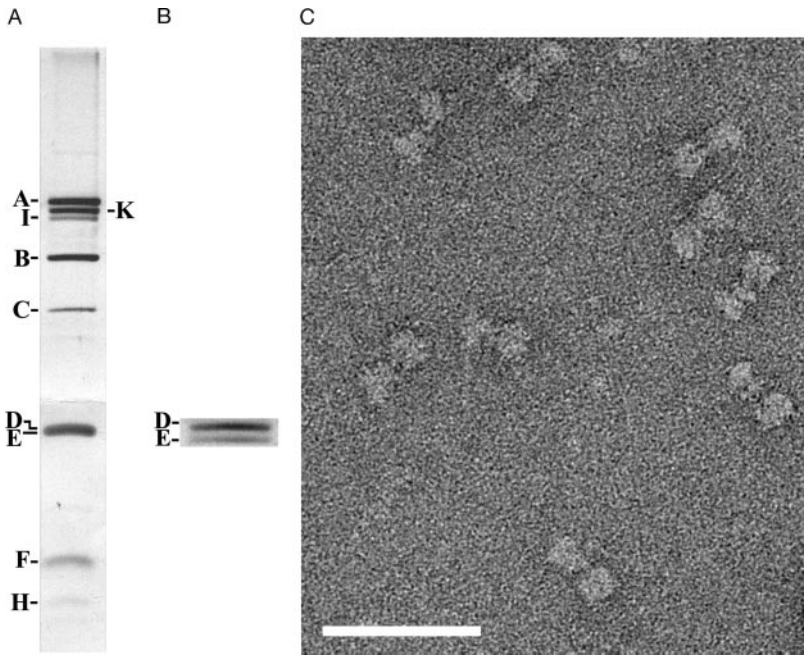

FIG. 1. **SDS-PAGE of isolated A_1A_0 ATP synthase from *M. jannaschii* and an electron micrograph of the negatively stained complex.** *A*, A_1A_0 ATP synthase was applied to SDS-PAGE (10%). To separate the subunits D (25 kDa) and E (23 kDa), the enzyme was loaded on a 17.5% gel (*B*). Both gels were stained with silver. The K-oligomer is SDS-resistant as shown recently (11) (*C*). *Bar* represents 50 nm.

resulted in a model in which the subunits C, D (partly), and F form the central stalk domain (7).

However, in contrast to the related F- and V-type ATP synthases/ATPases, little is known regarding the overall structure of the A_1A_0 molecule, which is largely due to the instability of the isolated complexes (10). Most recently, an isolation procedure of the A_1A_0 ATP synthase of the hyperthermophilic Archaea *Methanococcus jannaschii* resulted in a complete and functionally coupled enzyme (11). Besides the property of being an enzyme of a hyperthermophilic organism whose multienzyme complexes are believed to be more stable than those of mesophiles, the *M. jannaschii* A_1A_0 ATP synthase is of particular interest because it has a K subunit three times the size of that of most bacteria and Archaea. Furthermore, this subunit has lost one of the ion translocating residues (12). Here, we used electron microscopy to visualize directly the structure of the A_1A_0 ATP synthase from *M. jannaschii*. A comparison with the low resolution structure of the A_1 ATPase from *M. mazei* Gö1, derived from small-angle x-ray scattering data and single particle electron microscopy, allowed the unambiguous identification of most of the densities in the stalk domain and the A_0 part. The structure of the complete A_1A_0 ATP synthase also facilitates, for the first time, a comparison with structural models of the related F_1F_0 ATP synthase and V_1V_0 ATPase holoenzymes.

EXPERIMENTAL PROCEDURES

Materials—All of the chemicals were of reagent grade and were obtained from Merck (Darmstadt, Germany), BIOMOL (Hamburg, Germany), Roth (Karlsruhe, Germany), or Sigma (Deisenhofen, Germany).

Protein Preparation—The A_1A_0 ATP synthase of *M. jannaschii* was purified by sucrose density centrifugation and anion-exchange chromatography (DEAE-Sepharose) as described previously (11). ATPase-active fractions were pooled and concentrated on Centricon 100-kDa concentrators (Millipore). The concentrated sample was loaded on a Superose 6 column (10/30, Amersham Biosciences) and eluted with 50 mM Tris-HCl (pH 7.5), 5 mM MgCl, 10% glycerine, 150 mM NaCl, 0.1% Triton X-100, 0.1 mM phenylmethylsulfonyl fluoride, and Pefabloc SC (a final concentration of 1 mM, BIOMOL). The peak fractions, which were stained with silver, were collected and analyzed by SDS-PAGE (13, 14). Mg^{2+}-dependent ATPase activity was determined as described earlier (15).

Electron Microscopy and Image Analysis—Protein was prepared on freshly glow-discharged carbon-coated copper grids stained with 2% uranyl acetate. Images of the negatively stained A_1A_0 ATP synthase were collected on a Philips CM20FEG electron microscope operating at 200 kV and liquid N_2-cooled specimen to reduce radiation damage. Images of 2,048 × 2,048 pixels (after a binning of 2) were recorded at ×67,200 magnification at a pixel size of 30 μm with a Gatan 4000 SP 4K slow-scan CCD camera with GRACE software for semi-automated specimen selection and data acquisition (16). Single particle analysis was performed with the GRIP (Groningen image processing) software package on a PC cluster.[2] A total of 17,238 single particle projections (128 × 128 pixel frame; pixel size of 0.34 nm) from 331 images were obtained by selecting all of the discernable particles. For each micrograph, the defocus value was determined and a simple contrast transfer function correction by phase reversal was done (17). After band-pass filtering, the images were subsequently subjected to multireference alignment, multivariate statistical analysis, and hierarchical ascendant classification. This dataset was divided into two subsets including either one or two peripheral stalks to obtain a more homogenous dataset for a refinement of these classes. The subsets were analyzed in parallel by reference-free alignment (18). Each rotational and translational alignment was repeated four times, and classification was done by multivariate statistical analysis. Datasets were again divided and aligned as described above. The final classification of the homogenous datasets was performed by multivariate statistical analysis and hierarchical classification to extract the key structural features of the enzyme (19). The resolution of the class averages was measured according to van Heel (20).

RESULTS

Subunit Composition and Electron Microscopy—A characteristic gel of the preparation of the A_1A_0 ATP synthase from *M. jannaschii* is presented in Fig. 1*A* showing the nine subunits, A–F, H, I, and K, with apparent molecular masses of 66, 51, 45, 25, 23, 11, 10, 77, and 21 kDa, respectively. A typical electron microscopy raw image of the enzyme yields monodisperse particles with almost no contamination by smaller particles that could represent dissociated complexes or fragments (Fig. 1*B*). A total of 17,238 such molecular images were subjected to image processing. Fig. 2 demonstrates different class sums of the A_1A_0 ATP synthase projections obtained after several steps of reference-free translational/rotational alignment, multivariate statistical analysis, and multireference alignment. All of the projections reveal a tripartite structure consisting of a headpiece, a membrane-embedded domain, and a connecting stalk region. The classes can be grouped in respect

[2] W. Keegstra, unpublished data.

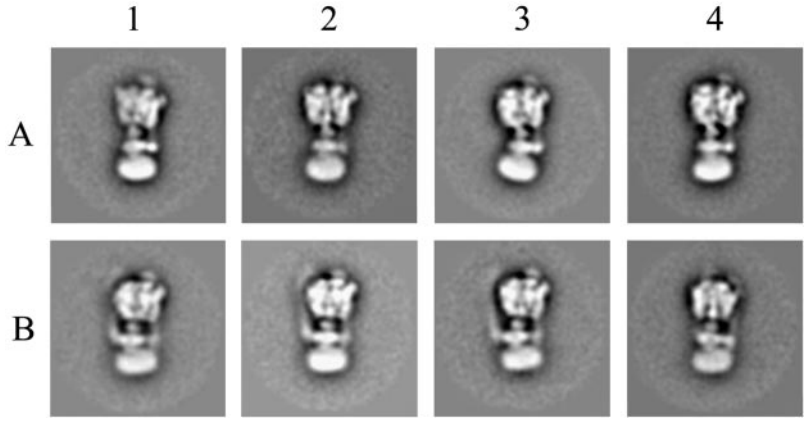

FIG. 2. **A gallery of selected classes resulting from the last multivariate statistical analysis and classification of 17,238 particles of the A_1A_0 ATP synthase.** Four classes (1–4) showing either one (*A*) or two (*B*) peripheral stalk(s) besides the central stalk are shown.

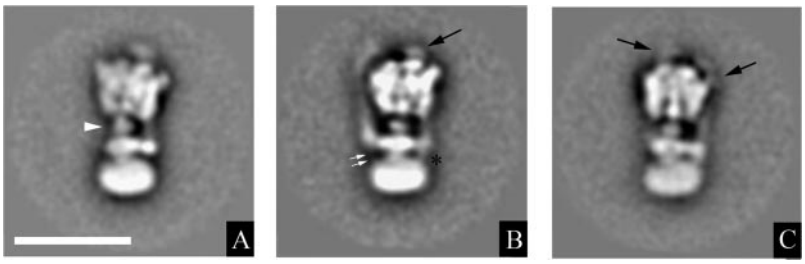

FIG. 3. **Total averages calculated from 410 (*A*), 497 (*B*), and 316 (*C*) images.** *C*, a projection at around 40° compared with that in *B*. *Bar* represents 20 nm. Labels: *black arrows*, masses of the peripheral stalks connected with the A_1 headpiece; *white arrowhead*, asymmetric upper part of the central stalk; *black asterisk*, mass connecting the A_0 with the collar like domain; *white arrows*, mass extending from the collar and the A_0 domain.

to the number of visible stalks: one group showing one peripheral stalk besides the central stalk (Fig. 2, *frames A1–4*; 12,555 particles) and a second group with two peripheral stalks on both the left and right side (Fig. 2, *frames B1–4*; 4,683 particles). To obtain more homogeneous classes, both data sets, including either two or three stalks, were analyzed separately as described under "Experimental Procedures." Fig. 3 shows averages of each refined data set at a resolution of 1.8 nm (Fig. 3, *A–C*). In all of the averages, the A_1A_0 ATP synthase from *M. jannaschii* has a total length of 25.9 nm. The dimensions of the A_1 headpiece, the central stalk domain, and the membrane portion, A_0, are 9.4 × 11.5, 8.0 × 3.9, and 6.4 × 10.6 nm, respectively. The A_1 headpiece has a rather spherical mass that is clearly separated from the stalk domain at its base (Fig. 3*B*). The stalk domain is formed by a central stalk and either one (Fig. 3*A*) or two peripheral stalks (Fig. 3*B*). This observation might be explained either by some of the complexes being disrupted or by these classes containing complexes in different orientation. The central stalk can be divided into an asymmetric upper part and a collar-like structure located above the A_0 domain. In the collar, several distinct densities could be resolved. At both ends of this domain, two of such densities are connected to the peripheral stalks (Fig. 3*B*), which go all the way up to the A_1 headpiece. One of these stalks appears to be in close contact with two areas of the A_1 headpiece with one located at the outside and the second located on top of the A_3B_3 headpiece (Fig. 3, *B* and *C*). This peripheral stalk shows a clear connection to the A_0 portion via the collar structure (Fig. 3, *B* and *C*). By comparison, the second peripheral stalk is attached to the top of the A_1 headpiece (Fig. 3*C*) and extended slightly down from the collar domain (Fig. 3*B*). A corresponding weak density rises up from the A_0 (Fig. 3*B*). Whereas the peripheral stalk(s) seems to be connected to the outside of the A_0 domain, the central stalk is attached to the center of the membrane-embedded A_0, which appears as a rather symmetric flattened sphere and slightly tilted in most of the projections, especially in Fig. 2, *frame B3*.

Localization of the Subunits Inside the A_1A_0 ATP Synthase—A known three-dimensional reconstruction of the asymmetrical A_1 complex from *M. mazei* Gö1 (7) determined from tilt pairs of negatively stained molecules was superimposed on the projection of the A_1A_0 ATP synthase from *M. jannaschii* (Fig. 4, *panel C*) by rotating the A_1 subcomplex in 5° steps through 360°. One of the projections of the A_1 from *M. mazei* Gö1 is well accommodated within the A_1 headpiece, composed of the A_3B_3D subassembly (7) and the upper central stalk, which is only partially (35%) solved in the three-dimensional reconstruction of the A_1 ATPase from *M. mazei* Gö1 (7). In this projection, one of the catalytic A subunits is on the right of the A_1 domain, implying that the peripheral stalk on the right may be close to this major A subunit. Nevertheless, from the superposition of the A_1 profile with the A_1 part in the A_1A_0 ATP synthase images, it is clear that the cap at the top of the A_1 headpiece (Figs. 3*B* and 4*C*) does not belong to the A_3B_3D subassembly. To further examine the composition of the central stalk, the projection of the A_1A_0 ATP synthase from *M. jannaschii* was compared with the solution structure of the A_3B_3CDF complex of the A_1 ATPase from *M. mazei* Gö1 deduced from solution x-ray scattering data (8). The central stalk of the hydrated A_3B_3CDF complex, which consists of the subunits C, F, and a part of subunit D, is 8.4 nm in length (8) and fits well to the dimensions (8 nm) of the elongated central stalk of the negative-stained A_1A_0 ATP synthase, indicating that the central stalk is made up by the subunits C, D (partly), and F.

DISCUSSION

The A_1A_0 ATP synthase has been described as a chimeric enzyme combining the structural and functional features of F_1F_0 ATP synthases and V_1V_0 ATPases (4). Single particle analysis resulted in the visualization of projections of the A_1A_0 ATP synthase from *M. jannaschii* consisting of an A_1 headpiece and an A_0 domain linked by a central stalk and two peripheral stalks. The A_1 headpiece fits well with the projection of the recently determined three-dimensional reconstruction with the A_1 complex from *M. mazei* Gö1 composed of the hexagonal A_3B_3 domain surrounding a cavity in which the central stalk subunit D is located (7, 8). The subunit is displaced toward an A-B-A triplet (7), allowing the rearrangements of the central D sub-

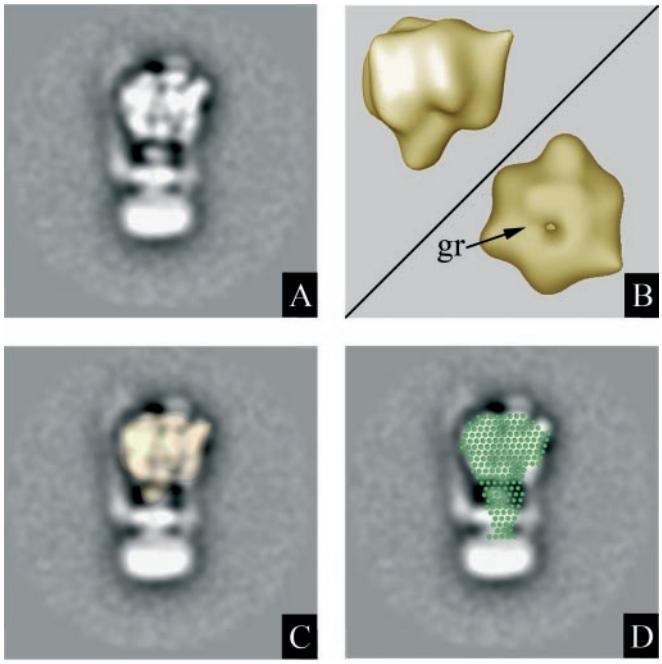

FIG. 4. *A*, *C*, and *D*, comparison of the A_1A_0 ATP synthase from *M. jannaschii* (*A*) with the projection of the three-dimensional reconstruction of the A_1 complex (*C*) (7) and the low resolution structure of the hydrated A_3B_3CDF complex (*D*) (8) from *M. mazei* Gö1. *B*, *side* and *top view* of the surface representation of the three-dimensional reconstruction of the A_1 ATPase from *M. mazei* Gö1 at a 3.2-nm resolution (7). The *black arrow* points at the groove of the A_1 headpiece. The *side view* of the A_1 complex (*gold*; *C*) and the envelope of the hydrated A_3B_3CDF complex derived from small-angle x-ray scattering data (*green*; *D*) from *M. mazei* Gö1 are superimposed on the projection of the A_1A_0 ATP synthase from *M. jannaschii*, respectively.

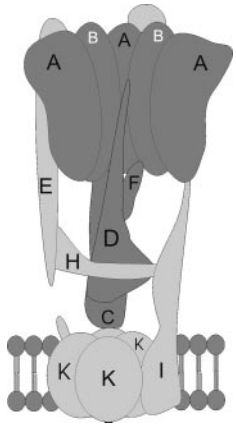

FIG. 5. **Model of the subunit topology in the A_1A_0 ATP synthase from *M. jannaschii*. A_1 and A_0 subunits are labeled in *dark* and *light grey*, respectively.** The subunit topology in the A-type ATP synthase is based on biochemical (6–8) and structural data (Refs. 8, 9, and this work). The triplicated proteolipids of *M. jannaschii* arose by gene triplication followed by a fusion of the gene copies and resulting in the proposed stoichiometry of four K subunits (4).

unit as demonstrated for the A_1 ATPase from *M. mazei* Gö1 (6, 7) and the related *Thermus thermophilus* A_1/V_1 ATPase (21). A key feature from the superposition of the A_1 complex from *M. mazei* Gö1 and the A_1A_0 ATP synthase is the close fit at the top of the A_1 headpiece showing the knoblike structures. These knobs, also found in the related V-type ATPase (22–25) but absent in the F-type ATP synthases (26–28), are formed by the N-terminal non-homologous inserts (80–90 amino acids) of the three catalytic A subunits, which alternate with the nucleotide-binding B subunits (7, 29). They point out that the cap at the very top of the A_1A_0 molecule (Fig. 4*C*) is not formed by a subunit belonging to the soluble A_1 domain (see below).

The comparison of the A_1A_0 ATP synthase with the recently determined envelope of the *M. mazei* Gö1 A_3B_3CDF complex in solution (8) yields that there is no significant shrinkage of the A_1A_0 molecule through the negative staining procedure. The central stalk is rather elongated (~8 nm) and in close contact with A_0. As described recently, the central stalk of the *M. mazei* Gö1 A_3B_3CDF complex accommodates subunits C, F, and partly D (7, 8). The cross-linking data of this complex indicate that subunit F is in close neighborhood to one of the nucleotide-binding B subunits (Fig. 5) and that F, together with the central stalk subunits C and D, undergoes significant structural rearrangements depending on nucleotide binding (6, 7). Such nucleotide-dependent alterations of stalk subunits C, D, and F will facilitate the mechanistic linkage of ATP synthesis/hydrolysis in the A_3B_3 hexamer to ion pumping in the A_0 part via the central CDF stalk domain. The length and the shape of the central stalk of the A_1 part resemble those of the related V_1 ATPase (8, 9). In contrast, the central stalk of the complete bacterial F_1 ATPase is substantially shorter (4.0–4.5 nm) (9, 30).

The question that now arises is, which subunits of the A_1A_0 ATP synthase contribute to the A_0 domain, the peripheral stalks, and the additional mass on top of A_1. The A_1A_0 ATP synthase as isolated has nine subunits (A–I, K). Five of them form the A_1 part and are assembled in the stoichiometry A_3B_3CDF (see above). The I and K subunits form the membrane domain, A_0 (11, 12). Subunit I (70 kDa) is very similar to subunit a of V_1V_0 ATPases with a hydrophilic N-terminal and a hydrophobic C-terminal domain. The C terminus of subunit I is predicted to have seven transmembrane helices and is assumed to be functionally similar to subunit a of the V_1V_0 ATPases and F_1F_0 ATP synthases (3). The N-terminal domain is predicted to be highly α-helical and assumed to be the functional homolog of the soluble domain of peripheral stalk subunit b of F_1F_0 ATP synthases. Because only one of the peripheral stalks is clearly attached to the outside of the A_0 domain, we conclude that the hydrophilic N terminus of subunit I emerges from the membrane-embedded A_0 part and may go up along the side of A_1 until the top of the A_1 headpiece (Fig. 5). Whether the N-terminal domain might partly contribute to the cap on the top of the A_1A_0 molecule can only be speculated. In the presented average, the peripheral stalk (*right*) has a kinked structure in the lower part, giving this domain the flexibility to wrap around the A_1 headpiece and ending up as the cap on the top (Fig. 3, *B* and *C*). Insertion and deletion of altered length in the so-called "tether" domain of the peripheral stalk subunit b of the *Escherichia coli* F_1F_0 ATP synthase, which is located above the membrane service, can be tolerated by the enzyme, indicating that this related connecting stalk has an inherent flexible structure (31). It has been suggested for the F_1F_0 ATP synthases that flexibility of the domain might allow reorientation of the stalk to act as a stator for rotation in one direction during ATP synthesis and in the opposite direction during ATP hydrolysis (31, 32).

Subunit K is a homolog of the F-type subunit c with two transmembrane helices. It consists of fused tandem repeats of sequences corresponding to the F-type subunit. *M. jannaschii* has a subunit K with six membrane-spanning helices (27 kDa) but with only two active carboxylates per monomer (12), which are involved in ion conduction along the membrane. As in the case of the F-type ATP synthases (33, 34) and V-type ATPases (35), the K subunits (or c in the F- and V-type ATPases) are thought to form a ring, which belongs to the rotary element inside the A_1A_0 ATP synthase. As shown in Fig. 4, the bottom of the central CDF-stalk domain spans the upper center of the A_0 domain, facilitating the direct contact of the rotary ele-

ments, which consists of an ensemble made from the central stalk (CDF domain) and a ring of hydrophobic K subunits in the A_0 membrane domain (21).

The second peripheral stalk appears to be connected to the collar domain and goes up to the A_1 headpiece. Probable candidates for this stalk are the remaining A_1A_0-hydrophilic subunits H (12 kDa) and E (25 kDa) with the latter predicted to be highly α-helical (12). The modest contact area of this peripheral stalk with the A_1 headpiece, which is also evident in electron micrographs of the related bacterial V_1V_0 ATPase from *Caloramator fervidus* (36), might be caused partially by stain accumulation. The top view projection of the rotated A_1 complex (Fig. 4, *panel D*) shows a groove at the top of the A_3B_3-hexamer in close neighborhood to this peripheral stalk. Such a groove-like feature may form a binding domain for the peripheral connection in the A_1 headpiece. In general, the positions of the peripheral stalks of the A_1A_0 ATP synthase as deduced from side views cannot be directly verified from top view projections, because such projection are not present in significant numbers if intact A_1A_0 molecules are prepared.

In summary, the first two dimensional projection maps of the A_1A_0 ATP synthase from *M. jannaschii* presented provides the structural basis toward a fuller understanding of the mechanistic events occurring in this class of enzymes. The reconstruction at a 1.8-nm resolution shows similarities and diversities between the structural modules to the evolutionary-linked F_1F_0 ATP synthases and V_1V_0 ATPases, such as the catalytic $A_1/F_1/V_1$ headpiece and the central stalk domain. Although the existence of one (26, 37) or two (27) peripheral stalk(s) in the F_1F_0 ATP synthase is uncertain, these classes of ATPases/synthases might need at least one peripheral stalk acting as a stator that prevents the major hexameric arranged subunits ($\alpha_3\beta_3$ or A_3B_3) from following the rotation of the central stalk domain. Whether the visualized second peripheral stalk in the V_1V_0 ATPase and in the presented A_1A_0 ATP synthase might act as a regulatory domain in the A-type ATP synthase as described for the plant V ATPase (25) can now be addressed.

REFERENCES

1. Yoshida, M., Muneyuki, E., and Hisabori, T. (2001) *Nat. Rev. Mol. Cell. Biol.* **2,** 669–677
2. Nelson, N. (1992) *Biochim. Biophys. Acta* **1100,** 109–124
3. Müller, V., Ruppert, C., and Lemker, T. (1999) *J. Bioenerg. Biomebr.* **31,** 15–28
4. Müller, V., and Grüber, G. (2003) *Cell Mol. Life Sci.* **60,** 474–494
5. Müller, V. (2004) *J. Bioenerg. Biomembr.* **36,** 115–125
6. Coskun, Ü., Grüber, G., Koch, M. H. J., Godovac-Zimmermann, J., Lemker, T., and Müller, V. (2002) *J. Biol. Chem.* **277,** 17327–17333
7. Coskun, Ü., Radermacher, M., Müller, V., Ruiz, T., and Grüber, G. (2004) *J. Biol. Chem.* **279,** 22759–22764
8. Grüber, G., Svergun, D. I., Coskun, Ü., Lemker, T., Koch, M. H. J., Schägger, H., and Müller, V. (2000) *Biochemistry* **40,** 1890–1896
9. Svergun, D. I., Konrad, S., Huss, M., Koch, M. H. J., Wieczorek, H., Altendorf, K., Volkov, V. V., and Grüber, G. (1998) *Biochemistry* **37,** 17659–17663
10. Wilms, R., Freiberg, C., Wegerle, E., Meier, I., Mayer, F., and Müller, V. (1996) *J. Biol. Chem.* **271,** 18843–18852
11. Lingl, A., Huber, H., Stetter, K. O., Mayer, F., Kellermann, J., and Müller, V. (2003) *Extremophiles* **7,** 249–257
12. Ruppert, C., Kavermann, H., Wimmers, S., Schmid, R., Kellermann, J., Lottspeich, F., Huber, H., Stetter, K. O., and Müller, V. (1999) *J. Biol. Chem.* **274,** 25281–25284
13. Schägger, H., Cramer, W. A., and v. Jagow, G. (1994) *Anal. Biochem.* **217,** 220–230
14. Damerval, C., le Guillioux, M., Blaisomeau, J., and de Vienne, D. (1987) *Electrophoresis* **8,** 158–159
15. Heinonen, J. K., and Lahti, R. J. (1981) *Anal. Biochem.* **113,** 313–317
16. Oostergetel, G.T., Keegstra, W., and Brisson, A. (1998) *Ultramicroscopy* **74,** 47–59
17. Frank, J., and Penczek, P. (1995) *Optik* **98,** 125–129
18. Dube, P., Bacher, G., Stark, H., Mueller, F., Zemlin, F., van Heel, M., and Brimacombe, R. (1998) *J. Mol. Biol.* **279,** 403–421
19. van Heel, M., and Frank, J. (1981) *Ultramicroscopy* **6,** 187–194
20. van Heel, M. (1984) *Ultramicroscopy* **13,** 165–184
21. Imamura, H., Nakano, M., Noji, H., Muneyuki, E., Ohkuma, S., Yoshida, M., and Yokoyama, K. (2003) *Proc. Natl. Acad. Sci. U. S. A.* **100,** 2312–2315
22. Boekema, E. J., Ubbink-Kok, T., Lolkema, J. S., Brisson, A., and Konings, W. N. (1998) *Photosyn. Research* **57,** 267–273
23. Wilkens, S., Vasilyeva, E., and Forgac, M. (1999) *J. Biol. Chem.* **274,** 31804–31810
24. Grüber, G., Radermacher, M., Ruiz, T., Godovac-Zimmermann, J., Canas, B., Kleine-Kohlbrecher, D., Huss, M., Harvey, W. R., and Wieczorek, H. (2000) *Biochemistry* **39,** 8609–8616
25. Domgall, I., Venzke, D., Luttge, U., Ratajczak, R., and Böttcher, B. (2002) *J. Biol. Chem.* **277,** 13115–13121
26. Wilkens, S., and Capaldi, R. A. (1998) *Biochim. Biophys. Acta* **1365,** 93–97
27. Böttcher, B., Bertsche, I., Reuter, R., and Gräber, P. (2000) *J. Mol. Biol.* **296,** 449–457
28. Karrasch, S., and Walker, J. E. (1999) *J. Mol. Biol.* **290,** 379–384
29. Grüber, G., Wieczorek, H., Harvey, W. R., and Müller, V. (2001) *J. Exp. Biol.* **204,** 2597–2605
30. Grüber, G. (2000) *J. Bioenerg. Biomembr.* **32,** 341–346
31. Grabar, T. B., and Cain, B. D. (2003) *J. Biol. Chem.* **37,** 34751–34756
32. Hardy, A. W., Grabar, T. B., Bhatt, D., and Cain, B. D. (2003) *J. Bioenerg. Biomembr.* **35,** 389–397
33. Stock D., Gibbons C., Arechaga I., Leslie A. G., and Walker, J. E. (2000) *Curr. Opin. Struct. Biol.* **10.** 672–679
34. Vonck, J., von Nidda, T. K., Meier, T., Matthey, U., Mills, D. J., Kühlbrandt, W., and Dimroth, P. (2002) *J. Mol. Biol.* **321,** 307–316
35. Wilkens, S., and Forgac, M. (2001) *J. Biol. Chem.* **276,** 44064–44068
36. Boekema, E. J., van Bremen, J. F. L., Brisson, A., Ubbink-Kok, T., Konings, W. N., Lolkema, J. S. (1999) *Nature* **401,** 37–38
37. Rubinstein, J. L., Walker, J. E., and Henderson, R. (2003) *EMBO J.* **22,** 6182–6192